THE SHEAR CAPACITY AND IMPROVEMENT MEASUREMENTS OF RC SPECIALLY-SHAPED COLUMN JOINTS

PAN Wen[1] and GENG Yonghong[2]

[1] *Professor, Dept. of Civil Engineering , Kunming Univ. of Sci. & Tech., Kunming, China*
[2] *Engineer, Kunming Architectural Design and Research Institute, Co., Ltd, Kunming, China*
Email: panwen@vip.sina.com

ABSTRACT :

The joint shear capacity of RC specially-shaped column (SSC) structures in high intensity seismic zone was studied in this paper, and two measurements for improving joint shear capacity were put forward, there were vertical haunch in the beam end and embedded cold-formed steel in joint. ABAQUS software was employed for nonlinear finite element analysis of ordinary joints, joints with vertical haunch and with embedded cold-formed steel, taking tensile cracking, compressive crushing of concrete and yield of steel into account. Analysis results showed the improvement of shear capacity of joints with vertical haunch and with embedded cold-formed steel, revealed the change of failure mechanism and ductility, provided the foundation for practical design method.

KEYWORDS: specially-shaped column, RC frame, joint, shear capacity, improvement measurements

1. INTRODUCTION

Previous earthquakes both home and abroad revealed the weakness of the beam-column joints of the RC frame structure, which is one of the main causes of building damage [Tang, 1989]. RC frame structures with SSC have big ratio of column section height to width and crowd rebar in beam-column junctions, so the construction quality of joints is poorer than ordinary rectangular columns and the earthquake damage may be more serious. Improvement of shear capacity of frame structures with SSC is of great significance for its extensive application. In this paper, two measurements for improving joint shear capacity were put forward, there were embedded cold-formed steel in joint (SRC joints) and vertical haunch in the beam end.

The section size of SRC joints is same as ordinary RC joints, and vertical haunch in the beam end could be as wide as partition wall and so be invisible.

Finite element (FE) method was employed for nonlinear analysis of joint damage process and capacity improvement mechanism of two measurements mentioned above.

2. DESCRIPTION OF FINITE ELEMENT MODEL

In order to analyze the stress and strain distribution, nonlinear damage process of ordinary SSC joints and SSC joints with SRC and vertical haunch, FE models with solid elements were established using ABAQUS software, as shown in figure 1 to 3.

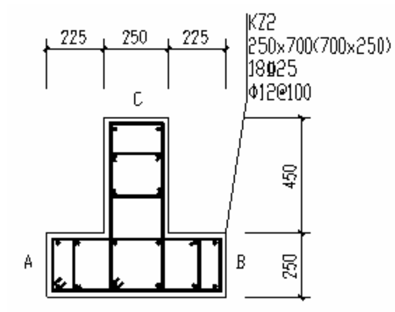

Fig.1 Ordinary SSC joint

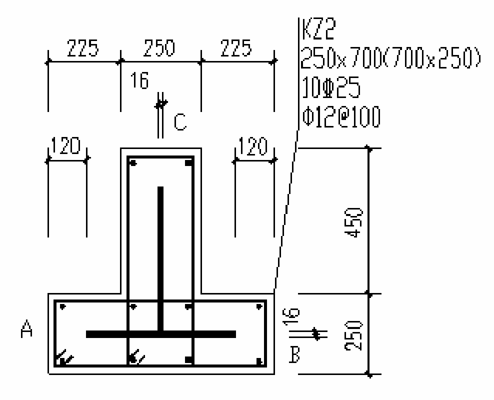

Fig.2 SSC joint with cold-formed steel

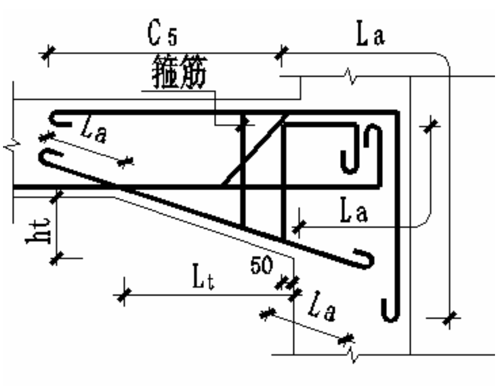

Fig.3 SSC joint with vertical haunch

The concrete in all models and cold-formed steel in SRC model were simulated by space hexahedral 8-node elements, longitudinal rebar and hoop were simulated by space 2 node elements, named as C3D8R and T3D2 in ABAQUS respectively [HKS, 2002]. The connection between concrete and rebar was taken as rigid and bond slip was ignored, that means concrete elements, longitudinal rebar and hoop share same nodes. Contact between concrete and cold-formed steel was taken into account by Coulomb friction. A rigid pad is attached in the SSC bottom (Figure 4), acted as boundary condition and avoided the inauthentic stress concentration near the fixed ends in usual FE models.

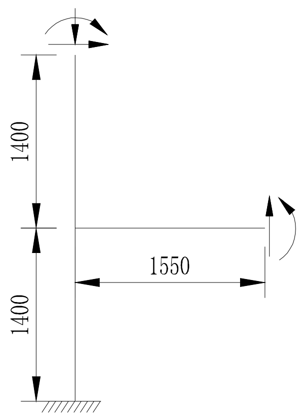

Fig.4 Joint nomogram

The joints concerned were taken from previous researches [Pan, et al., 2008]. The loads acted on the model and section reinforcement were obtained from routine design. The initial loads in the beam were: MA=-21.87KN.M, VA=109.08KN, MB=59.93KN.M, VB=62.31KN, MC=60KN.M, VC=150KN (subscript A, B, C marked beam ends, see Fig. 2); column initial loads were: axial force N=-441.61KN, MX=3.23KN.M, VX=63.45KN; MY=-5.818KN.M, VY=141.98KN (x, y marked directions in the Cartesian coordinate system). Because time is proportional to the load, the time step was utilized to represent load value and load history tracking parameters.

3. PRIMARY RESULTS FROM ANALYSIS

When FE models could not bear more load, i.e., calculation process in ABAQUS could not be convergent, the ultimate capacity of joint reached. The loads acted on the models were increasing in proportion from the initial value mentioned above.

3.1. Ordinary RC Joints

In early stage of loading until first cracking, the imposed load was approximately 30% of the ultimate load. Maximum principal stress of concrete was shown in figure 5. Firstly, concrete in the tension zone in the end of beam C reached its tensile strength and cracks began to appear, the internal force of the concrete was transferred to the beam longitudinal reinforcement bar, so its stress increased faster in the beam end.

In the crack development stage, the load was approximately 40% of the ultimate load, concrete in the central part of beam C reached its tensile strength, and cracks emerged in this area. Due to tension force transferring from beam end, the core concrete was in tension along diagonal direction, and cracks emerged near the junction of beam and column. With the increase of load, cracks in the central part of beam C developed fast in vertical direction, and the scope of cracks increased along horizontal direction. The cracks within the joint core area were increasing, particularly along the diagonal direction, tallying with the compression mechanism [Park, 1975]. When loads were up to approximately 50% ultimate load, cracks in the beam A, B ends began to appear; when the load arrived 60%, the maximum principal stress of concrete at the joint is shown in Figure 6. Stress of reinforcement bars in the central tension area of beams grew rapidly, and the stress of longitudinal bars and hoops was smaller.

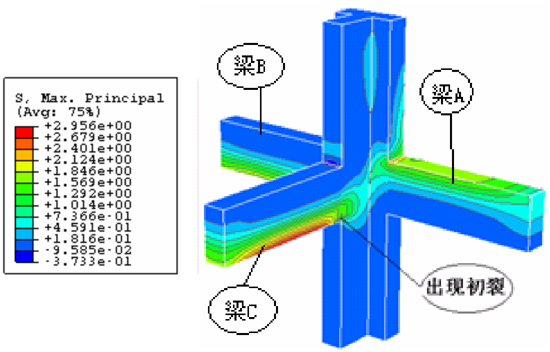

Fig.5 30% ultimate load, max principal stress

Chinese in picture are “beam A, B, C” and “first crack”

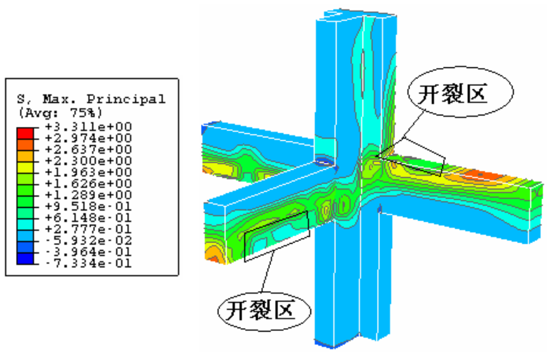

Fig.6 60% ultimate load, max principal stress

Chinese in picture is “cracked area”

Near the loads limit, with increase of the loads, the cracks in beam C developed continuous along vertical direction, and some concrete dropped out in the tension area. Cracks along the diagonal developed faster in the core and beam column junction, and there were cracking phenomenon in some tension areas of column, also some concrete dropped out in the beam A, B. Loading to the last step, the beam was damaged due to bent failure. At this time, the peak value of concrete stress was in beam C, 18.05 MPa, lower than compressive strength of concrete. State of maximum principal stress of concrete at last load step is shown in figure 7. The peak tensile stress of reinforcement bars was in the tension area of beam C, 184.1 MPa; and peak compressive stress was in the compressive area of beam C, -72.27 MPa. The largest tensile stress of hoop occurred in the junction of beam A and column, 135.2 MPa. State of maximum principal stress of reinforcement bars at last load step is shown in figure 8.

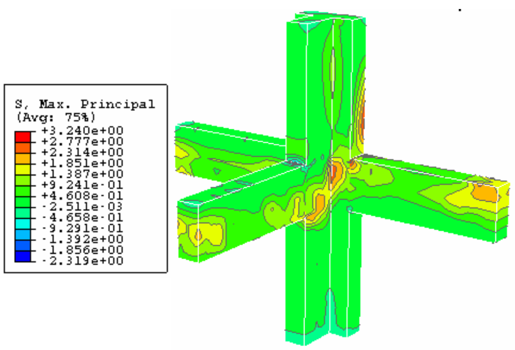

Fig.7 Ultimate load, max principal stress

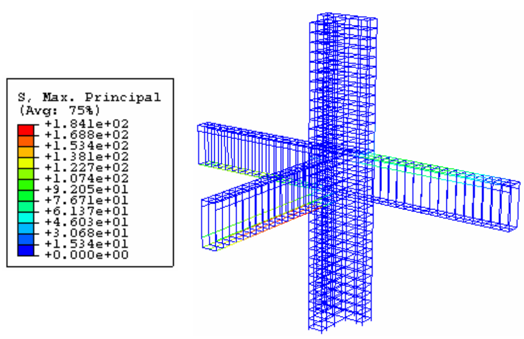

Fig.8 Ultimate load, max principal stress of rebar

3.2. SRC Joints

The final results of FE analysis showed that the ultimate capacity of SRC joint increased by 48%, comparing with ordinary RC joint, when section ratio of cold-formed steel was 5.04%. So, the ultimate load mentioned in this section was 1.48 times of above section.

When first crack occurred, the imposed load was approximately 30% of the ultimate load. Maximum principal stress of concrete was shown in Figure 9. Other phenomena were similar to RC joint, but first crack appeared near the mid span of beam, not the beam end.

In the crack development stage, when the load arrived 65% of the ultimate load (around the ultimate load of RC joint), the maximum principal stress of concrete at the joint is shown in figure 10. The peak tensile stress of reinforcement bars was in the tension area of beam C, 106.7.1 MPa; and peak compressive stress was in the compressive area of beam C, -47.8 MPa. The largest tensile stress of hoop in the joint core area was 68.4 MPa, far below its yield stress.

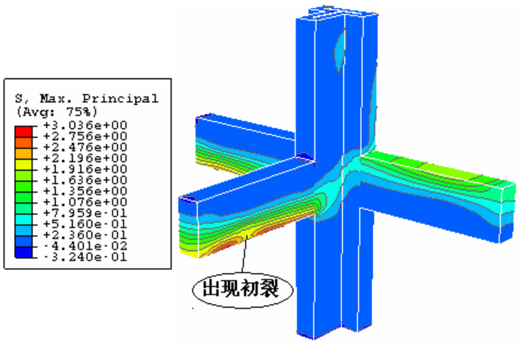

Fig.9 30% ultimate load, max principal stress

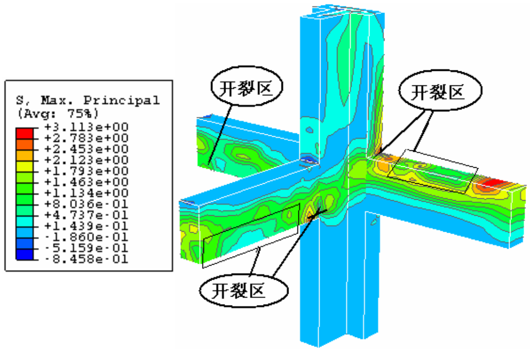

Fig.10 65% ultimate load, max principal stress

Near the loads limit, with increase of the loads, the cracks in beam C developed continuous along vertical direction, and some concrete dropped out in the tension area. Cracks appeared in the beam column junction, concrete in core area was in tensile state along the diagonal, but without crack, and tallying with the compression mechanism. Loading to the last step, the beam was damaged due to bent failure. At this time, the peak value of concrete stress was in beam C, 16.33 MPa, lower than compressive strength of concrete. State of maximum principal stress of concrete at last load step is shown in figure 11. The peak tensile stress of reinforcement bars was in the tension area of beam C, 195.21 MPa; and peak compressive stress was in the compressive area of beam C, -69.6 MPa. The largest tensile stress of hoop occurred in the junction of beam C and column, 103.1 MPa. State of maximum principal stress of reinforcement bars at last load step is shown in figure 12.

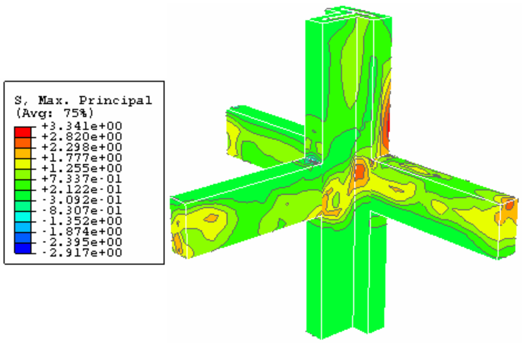

Fig.11 Ultimate load, max principal stress

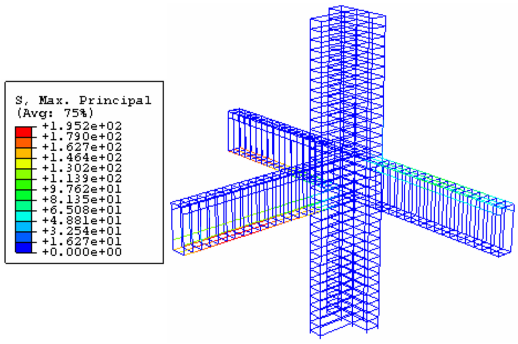

Fig.12 Ultimate load, max principal stress of rebar

The von Mises stress, maximum principal stress and shear stress of cold-formed steel embedded in the core were shown in figure 13-15, respectively. Cold-formed steel did not yield under the ultimate load, and was in a low stress level, since the failure of model was the result of bent failure of beam. From figure 15 it is obvious that the most part of total shear force acted on the cold-formed concentrated in the web, and in contrast, the flange shared a little. The reason could be that the distribution of total shear acted on the cold-formed steel between web and flange depends on the stiffness ratio of them, in the shear plane, web has a greater stiffness. Although flange has a little contribution to shear resistance, it transfers compressive and tensile force of beams and column directly to core area and reduces the stress level of concrete in the core area effectively; on the other hand, together with web, it constrains core concrete and provides better ductility and energy dissipation capacity.

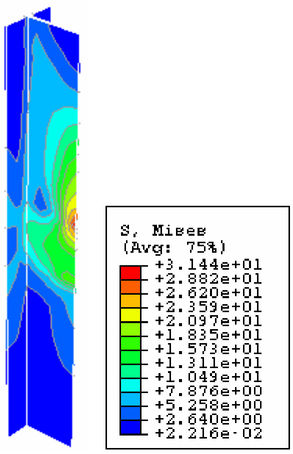

Fig.13 von Mises stress of cold-formed steel

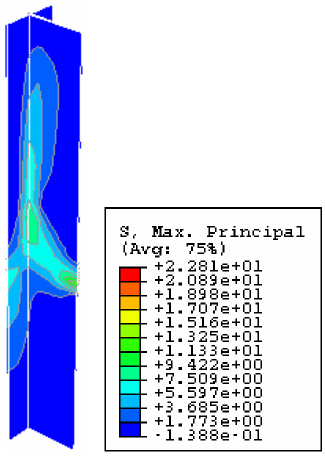

Fig.14 Max principal stress of cold-formed steel

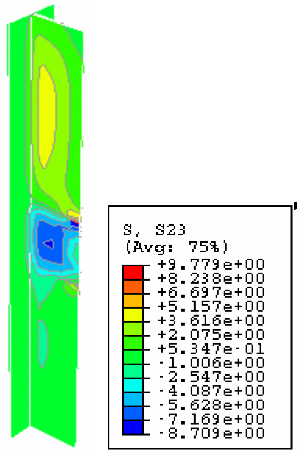

Fig.15 Shear stress of cold-formed steel

3.3. Haunched Joints

Except the embedded cold-formed steel, haunch in the beam end is also an effective method for improvement of shear capacity. The haunch means to add a wedge part under beam conjoint to the beam column junction. Obviously, beam haunch enlarges the height of beam and increases the shear capacity and stiffness. The final results of FE analysis showed that the ultimate capacity of joint with haunch increased by 29.8%, comparing with ordinary RC joint. So, the ultimate load mentioned in this section was 1.3 times of section 3.1.

As shown in figure 16, when first crack occurred in haunch end of beam conjunct to the web of T-shaped SSC, the imposed load was approximately 75.7% of the ultimate load (around the ultimate load of RC joint); when load imposed arrived 78.5%, 97.1% of the ultimate load, crack in haunch ends of other two beams conjunct to the flange of SSC appeared in sequence. The high stress zone in the beams moved away from the beam end to the midspan owing to the presence of haunch, and the stress increase of core was slackened. However, in the last stage of loading, the oblique cracks perpendicular to the direction of maximum principal stress appeared within the core area, and some of tensile force was transferred to rebars, tallying with the compression mechanism.

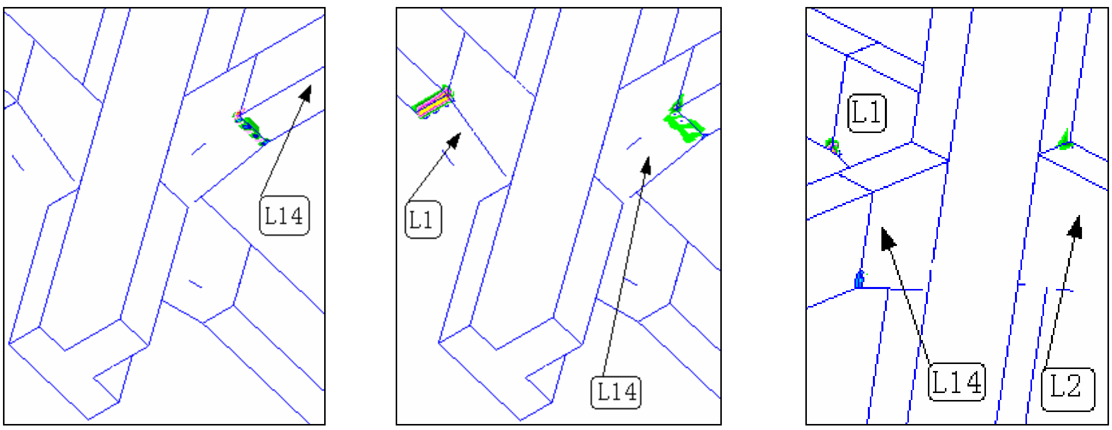

(a) 75.7% ultimate load　b）78.5% ultimate load　（c）97.1% ultimate load

Fig.16 Crack development of joints with beam haunch

The shear performance improvement of joints with beam haunch could be in virtue of the increase of core volume and section shear area, so the decrease of nominal shear stress. Additional, the increase of section height could decrease the amount of longitudinal rebars in the beam and core area, so improve the construction quality.

4. CONCLUSIONS

(1). Compared with the ordinary RC node, the load level of initial crack of SRC joint and joint with haunch increase by about 48% and 52%, the ultimate load by about 48% and 30%, respectively.

(2). For the RC joint, the plastic hinge appears in the end of beam. With the increase of load, the concrete cracks in tensile zone of beam develop and run through the whole section, bring on the failure of beam. Meanwhile, oblique cracks in diagonal direction in the core area enforce the compression mechanism and make the most of compressive capacity of core concrete. For SRC joint and joint with haunch, the plastic hinge appears away from the beam end due to the augment of core rigid zone. The core concrete stress states of them are similar to that of RC joint, but without crack in the core area. The embedded cold-formed steel and beam haunch participate in shear resistance of core, so decrease the core concrete stress.

(3). Longitudinal rebar stress distribution of three kinds of joint resembles, but that of SRC joint and joint with haunch is smaller than that of RC joint. Hoop strength of all joint does not exert effectively because the failure of joint is not due to the failure of core concrete but the bent failure of connected beam. The presence of hoops in the core restrains the width of cracks and shear strain of concrete, postpones the joint damage process.

(4). The joint shear capacity is a primary obstacle for extensive application of structures with SSC in high seismic intensity zones, embedded cold-formed steel and beam haunch could improve the shear capacity of beam-column joints effectively.

REFERENCES

HKS. (2002), ABAQUS/Standard User's Manual, Hibbitt, Karlsson & Sorensen, Inc

Pan Wen, Liu Jian, Yang Xiaodong. (2008). Shaking table test of 6-storey RC frame structure with specially shaped columns in seismic intensity zone 8, *Building Structure Journal*, in press. (in Chinese)

Park R. and Paulay T. (1975), Reinforced concrete structures, John Wiley & Sons, New York, USA

Tang Jiuru. (1989). New progress in seismic resistance of RC frame joints. Earthquake Resistant Engineering l989:4, 39-43. (in Chinese)